



Dominance of *Sulfurospirillum* in Metagenomes Associated with the Methane Ice Worm (*Sirsoe methanicola*)

Shen Jean Lim,^{a,b} Luke R. Thompson,^{b,c} Craig M. Young,^d Terry Gaasterland,^e Kelly D. Goodwin^b

^aCooperative Institute for Marine and Atmospheric Studies, Rosenstiel School of Marine and Atmospheric Science, University of Miami, Miami, Florida, USA

^bOcean Chemistry and Ecosystems Division, Atlantic Oceanographic and Meteorological Laboratory, National Oceanic and Atmospheric Administration, Miami, Florida, USA

^cNorthern Gulf Institute, Mississippi State University, Starkville, Mississippi, USA

^dOregon Institute of Marine Biology, University of Oregon, Eugene, Oregon, USA

^eBioinformatics and Systems Biology, University of California, La Jolla, California, USA

ABSTRACT *Sirsoe methanicola*, commonly known as the methane ice worm, is the only macrofaunal species known to inhabit the Gulf of Mexico methane hydrates. Little is known about this elusive marine polychaete that can colonize rich carbon and energy reserves. Metagenomic analysis of gut contents and worm fragments predicted diverse metabolic capabilities with the ability to utilize a range of nitrogen, sulfur, and organic carbon compounds through microbial taxa affiliated with *Campylobacteriales*, *Desulfobacteriales*, *Enterobacteriales*, *SAR324*, *Alphaproteobacteria*, and *Mycoplasmatales*. *Entomoplasmatales* and *Chitinivibrionales* were additionally identified from extracted full-length 16S rRNA sequences, and read analysis identified 196 bacterial families. Overall, the microbial community appeared dominated by uncultured *Sulfurospirillum*, a taxon previously considered free-living rather than host-associated. Metagenome-assembled genomes (MAGs) classified as uncultured *Sulfurospirillum* predicted thiosulfate disproportionation and the reduction of tetrathionate, sulfate, sulfide/polysulfide, and nitrate. Microbial amino acid and vitamin B12 biosynthesis genes were identified in multiple MAGs, suggesting nutritional value to the host. Reads assigned to aerobic or anaerobic methanotrophic taxa were rare.

IMPORTANCE Methane hydrates represent vast reserves of natural gas with roles in global carbon cycling and climate change. This study provided the first analysis of metagenomes associated with *Sirsoe methanicola*, the only polychaete species known to colonize methane hydrates. Previously unrecognized participation of *Sulfurospirillum* in a gut microbiome is provided, and the role of sulfur compound redox reactions within this community is highlighted. The comparative biology of *S. methanicola* is of general interest given research into the adverse effects of sulfide production in human gut microbiomes. In addition, taxonomic assignments are provided for nearly 200 bacterial families, expanding our knowledge of microbiomes in the deep sea.

KEYWORDS Gulf of Mexico, host-microbial interactions, invertebrate microbiology, metagenomics, methane hydrate, microbiome, polychaete, *Sulfurospirillum*, worm, deep-sea

Cold seeps are biologically productive deep-sea habitats that support distinct communities of organisms adapted to aphotic, high-pressure, and reducing conditions. Although various invertebrates have been identified at cold seeps, only *Sirsoe methanicola* (previously *Hesiocaeca methanicola*) is known to directly inhabit methane hydrates (1, 2) (Fig. 1). Methane ice worms possess a functional digestive system with a gut and are not known to possess epibionts or intracellular symbionts (2, 3).

The physical and biological mechanisms by which *S. methanicola* colonizes methane hydrates are unknown. Feeding studies suggested that free-living larvae feed on

Editor Isaac Cann, University of Illinois at Urbana-Champaign

This is a work of the U.S. Government and is not subject to copyright protection in the United States. Foreign copyrights may apply.

Address correspondence to Kelly D. Goodwin, kelly.goodwin@noaa.gov.

The authors declare no conflict of interest.

Received 18 February 2022

Accepted 16 May 2022

Published 12 July 2022

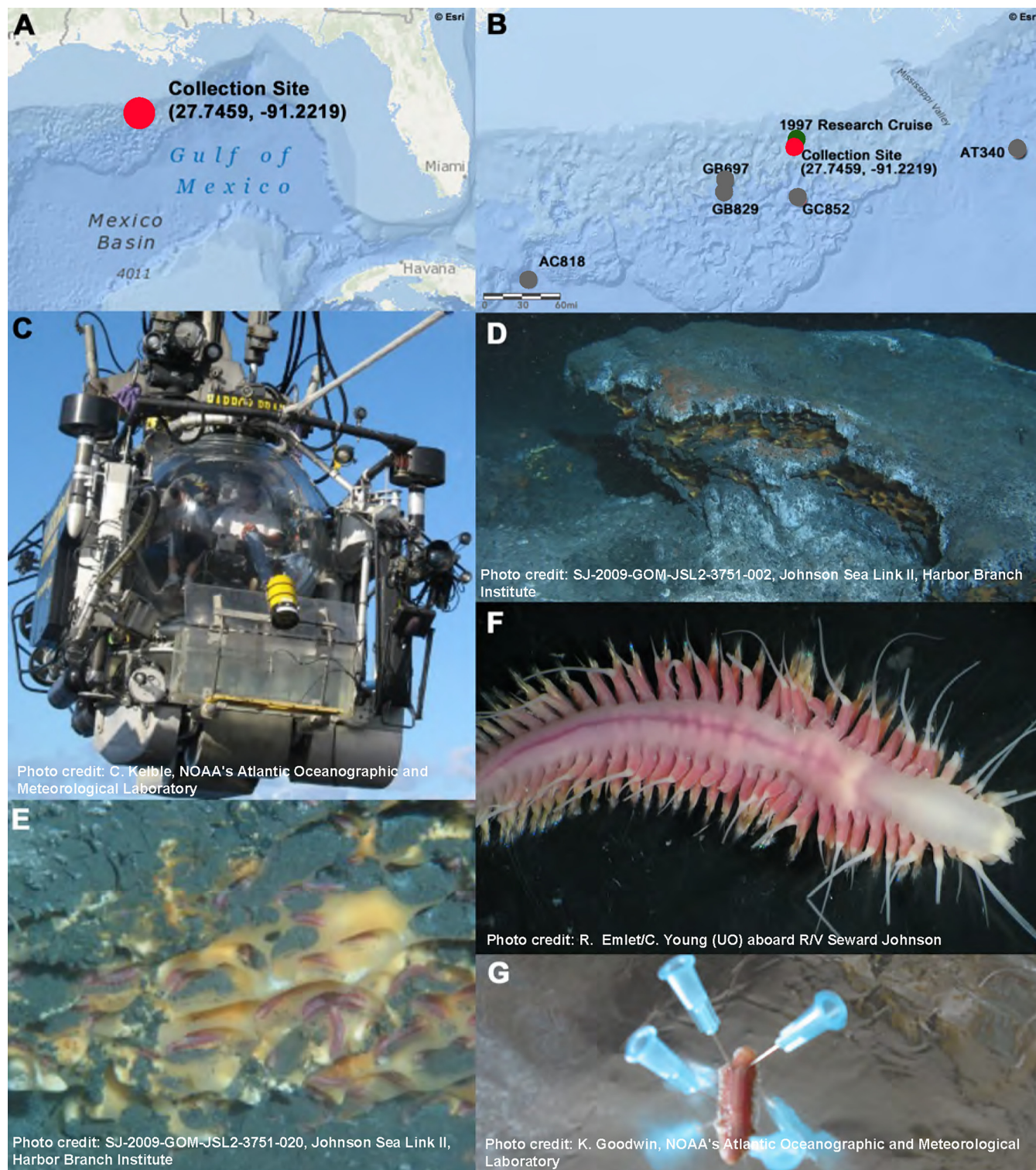


FIG 1 (A) Map showing location of collection site; (B) Zoomed in portion of map showing the collection site in this study (red circle) in relation to the site where *S. methanicola* was first discovered in 1997 (green circle) and sites AC818, GB697, GB829, GC852, and AT340 where *S. methanicola* specimens were sampled for stable isotope analysis (grey circles) (satellite data: Esri); (C) The *Johnson Sea-Link II* submersible used for sample collection; (D) Methane hydrate at the sampling site at 543m depth; (E) *S. methanicola* worms inhabiting depressions on the methane hydrate; (F) *S. methanicola* individual observed under the compound microscope; and (G) *S. methanicola* individual during aseptic dissection. AC, Alaminos Canyon; GB, Garden Banks; GC, Green Canyon; AT, Atwater Valley.

picoplankton, including heterotrophic bacteria, cyanobacteria *Prochlorococcus* and *Synechococcus*, and autotrophic picoeukaryotes $<3 \mu\text{m}$ (4). Several types of evidence, including average microbial densities for methane hydrates (4×10^6 cell/g to 2×10^7 cell/g), geochemical evidence, and stable isotope studies suggested that settled *S. methanicola* are bacterivores that feed on the surface of gas hydrates (2, 3, 5). Methanotrophs were not predicted to be a primary source of nutrition (3). Stable isotope studies suggested that the worm mainly obtained nitrogen, carbon, and sulfur from chemoautotrophic sulfur-oxidizing bacteria and may consume a variety of bacteria (2, 3).

More is known about the environmental microbiomes associated with methane hydrates compared to those associated with the worm itself. Previously sequenced clone libraries revealed that methane hydrate microbial communities were dominated by uncultured taxa. Archaeal 16S rRNA gene clone libraries from methane hydrate samples collected at Green Canyon (GC234) or Atwater Canyon in the Gulf of Mexico were dominated by anaerobic methanotrophic archaea (ANME) or closely affiliated methanogenic orders *Methanomicrobiales* and *Methanosarcinales* (6–8). Bacterial 16S rRNA gene clone libraries included sequences affiliated with *Deltaproteobacteria/Desulfobacterota* (5, 9), *Epsilonproteobacteria/Campylobacterota* (10), *Firmicutes*, *Chloroflexi*, and hydrocarbon-associated bacteria (5, 6). Other related taxa identified in this environment included *Bacteroidota* (*Cytophaga/Flavobacterium/Bacteroides*), *Spirochaetales*, *Verrucomicrobiales*, *Actinomycetales*, and *Thermus* (6, 8).

Methane hydrates can support microbial life through the slow release of gases, including methane, carbon dioxide, hydrocarbon gases, and hydrogen sulfide derived from microbial sulfate reduction in sulfate-containing porewater (5–7). The type of methane hydrates commonly found in the Gulf of Mexico region (Structure II) allow larger molecules such as ethane, propane, iso-butane, butane, and pentane to be trapped. The hydrate deposits can be rich in H_2S and may be stained with oil (2, 7, 11). The methane hydrate where *S. methanicola* was first discovered contained considerable amounts of thermogenic methane, hydrogen sulfide, hydrocarbon gases, and carbon dioxide (2).

Methane hydrates are ephemeral, and the collection of *S. methanicola* has been infrequent and serendipitous. As a result, little is known about this species. Here, we provided the first metagenomic sequencing analysis for *S. methanicola* to describe the taxonomy and functional potential of prokaryotes associated with this elusive deep-sea organism. The metabolic capacity of microbes living in association with *S. methanicola* was revealed by sequencing and assembling community DNA from gut contents and worm fragments.

RESULTS

Two HiSeq metagenomic libraries and one MiSeq library were created from live *S. methanicola* specimens retrieved from a Gulf of Mexico methane hydrate via a submersible (Fig. 1 and 2), with details provided in Table S1. Prokaryotic diversity and functional potential were assigned by a variety of analytical methods (Table S2), with a focus here on results obtained from the HiSeq libraries due to the higher coverage provided. Results of eukaryotic gene annotations, including mitogenome assemblies, are provided under separate cover (unpublished data).

Prokaryotic taxonomic composition from metagenomic reads. Thirteen prokaryotic full-length 16S rRNA gene sequences (1,069–1,558 bp; NCBI GenBank accession numbers [MZ229982](#) to [MZ229994](#)) were recovered through phyloFlash assembly (Table S2) of metagenomic sequences recovered from *S. methanicola* gut contents (Library G) and worm fragments (Library W). Sequence identity ranged from 82% to 100% based on BLAST searches (Table 1 and Table S3). Reads were most often affiliated with the full-length 16S rRNA gene sequence classified as uncultured *Sulfurospirillum* spp. (e.g., $>300,000$ reads for Library G), with $29\times$ more reads recruited from Library G and $3\times$ more reads from Library W compared to the next most abundant prokaryotic taxa. Other classifications associated with sulfur cycling bacteria included uncultured *Sulfurimonas* and *Desulfobacterales* (Table 1).

Additional best matches for these full-length sequences originated from various intestinal tracts and marine habitats (Table 1). These included uncultured *Mycoplasmataceae*,

Experimental design for metagenomic sequencing

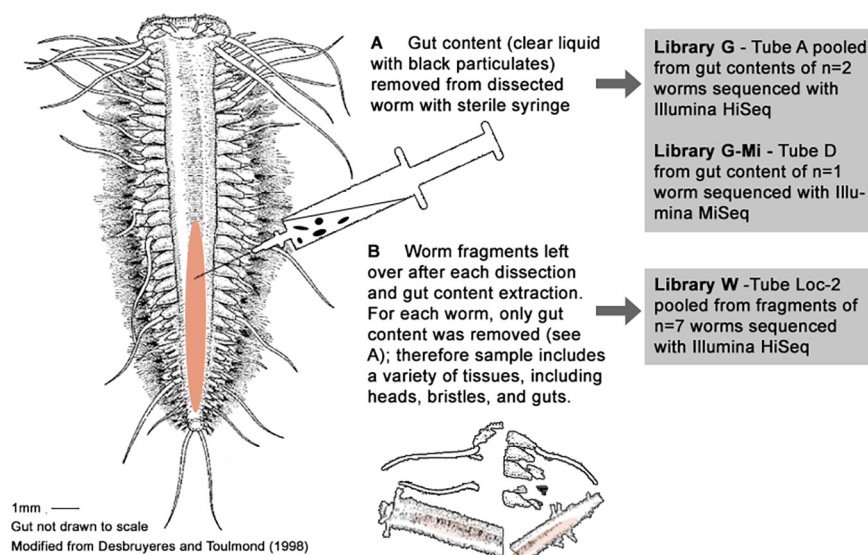


FIG 2 Experimental design used for metagenomic sequencing in this study. (A) Gut content was extracted with a sterile syringe. (B) worm fragments remaining after dissection and gut content extraction were collected. Libraries for metagenomic sequencing were created from samples of gut contents and worm fragments. Detailed descriptions of samples used to create Illumina HiSeq and MiSeq libraries and sequencing statistics are in Table S1. (The drawing of the dorsal view of the organism is reproduced from reference (1) with permission.)

Entomoplasmatales, *Vibrio*, *Chitinivibrionaceae*, and *Rhodospirillales*. Only one of the four full-length sequences recovered from Library W was unique (not shared with Library G), and it was assigned to the SAR324 clade. Two additional full-length sequences were recovered but rejected because sequences appeared chimeric (family *Desulfatiglans*) or showed low similarity to reference 12S rRNA gene sequences (order *Rickettsiales*). No full-length archaeal small subunit (SSU) rRNA sequences were extracted.

Metagenomic binning produced 16 bacterial metagenome-assembled genomes (MAGs) ($n = 12$, Library G; $n = 4$, Library W) (Table 2, Fig. 3, Table S4, and Data Set S2). In two instances, nearly identical MAGs were recovered from both libraries, with MAGs G15 and W8 classified as *Sulfurospirillum* and MAGs G3 and W7 phylogenetically related to uncultured *Alphaproteobacteria Rs-D84* recovered from a termite gut (Table S5). The nearly identical MAGs were combined and deduplicated for recruitment estimates.

The MAG identified as *Sulfurospirillum* (G15/W8) dominated read recruitment, recruiting 86% of the reads from library G and 59% of the reads from Library W. Read recruitment to the MAG classified as *Alphaproteobacteria Rs-D84* was 3% and 5% for libraries G and W, respectively (Table S4). Five of the recovered MAGs were classified in the order *Desulfobacterales* (G11, G19_1, G19_2, G10, and G16). Other MAGs were classified in the genera *Sulfurimonas* (G18), *Colwellia* (G12), and *Pseudoalteromonas* (G13), in the family *Sulfurovaceae* (G20), and in the orders *Mycoplasmatales* (W6), *Rickettsiales* (G4), and SAR324 (W9).

Most of the MAGs did not contain the extracted full-length 16S rRNA gene sequences (Table 1 and 2). The exceptions were MAG W7 classified as *Alphaproteobacteria Rs-D84* and MAG W9 classified as an uncultured member of the SAR324 cluster. The MAG classified as SAR324 recruited more reads from Library W than Library G (19% versus 0.05%; Table S4), consistent with a full-length 16S rRNA gene sequence extracted only from Library W.

PhyloFlash mapped a large number of reads to sequences in the SILVA database (12) ($n = 3926$, Data Set S3) in addition to generating the set of full-length 16S rRNA sequences (Table 1). We extended this analysis by mapping reads (mated paired-ends only) to a set of manually curated 16S rRNA gene sequences of uncultured taxa from methane hydrate and seep studies (Data Set S4). Again, taxonomic assignments were dominated by *Sulfurospirillaceae* (Table 3), all of which were assigned to the genus

TABLE 1 Read mapping results and bacterial taxonomic assignments of full-length 16S rRNA gene sequences generated by phyloFlash assembly of metagenomic libraries created from *S. methanicola* gut contents (G) and worm fragments (W) (Table S1 and S2)^a

| Library | No. reads | Coverage | PhyloFlash predicted taxonomy, dbHIT ^b (% identity; alignment length bp) | Accession, this study (bp) | NCBI megablast ^c (% identity; alignment length bp), source |
|----------------|-----------|----------|---|----------------------------|---|
| G | 482,632 | 1173.7 | o_Campylobacterales, f_Sulfurospirillaceae, g_Sulfurospirillum (uncultured), FJ717081.1.1505 (97.2; 1,490) | *MZ229985 (1,509) | FJ717081 (97.2; 1,503), lugworm (<i>Arenicola marina</i>) bioturbated mesocosm |
| W | 12,705 | 35.8 | | *MZ229991 (1,509) | |
| G | 2,949 | 8.1 | o_Campylobacterales, f_Sulfurimonadaceae, g_Sulfurimonas (uncultured), FJ717084.1.1513 (97.0; 1,499) | MZ229989 (1,517) | FJ717065 (97.6; 1,512), lugworm (<i>Arenicola marina</i>) bioturbated mesocosm |
| G | 1,035 | 3.4 | o_Desulfobacterales, f_Desulfosarcinaceae (uncultured) ^d , AXAM01000010.50040.5158 (99.7; 1,185) | MZ229990 (1,198) | HG513093 (98.1; 1165), Guaymas Basin sediments, butane enriched sulfate-reducing conditions |
| G | 268 | 1.2 | o_Desulfobacterales, f_Desulfosarcinaceae (uncultured), JF344525.1.1523 (99.1; 1,167) | MZ229982 (1,201) | JQ580155 (99.4; 1166), oil-polluted subtidal sediments |
| G | 5,634 | 15.1 | o_Mycoplasmatales, f_Mycoplasmataceae (uncultured), HG792201.1.1524 (91.5; 1,524) | *MZ229986 (1,558) | HG792201 (91.7; 1,521), Chinese mitten crab (<i>Eriocheir sinensis</i>) intestinal tract |
| W | 372 | 1.3 | | *MZ229994 (1,558) | |
| G | 5,787 | 18.6 | o_Entomoplasmatales, f_Entomoplasmatales <i>Incertae Sedis</i> , g_Candidatus <i>Hepatoplasma</i> (uncultured), HE610322.1.1517 (81.6; 1,498) | MZ229988 (1,515) | AY592891 (90.8; 1,141), cold seep mud volcano microbial mat |
| G | 535 | 1.8 | o_Enterobacteriales, f_Vibrionaceae, g_Vibrio, s_splendidus, CP031055.3036629.303808 (99.9; 1,057) | MZ229983 (1,069) | CP062501 <i>Vibrio bathopelagicus</i> (100; 1,069), Mediterranean Sea |
| G | 155 | 0.8 | o_Chitinivibrionales, f_Chitinivibrionaceae, GQ348358.1.1382 (93.3; 1,125) | MZ229984 (1,152) | GQ348358 (93.6; 1,132), Saanich Inlet |
| W ^e | 4,244 | 13.5 | SAR324 clade (Marine group B) (uncultured), EU101262.1.1465 (89.1; 1470) | MZ229993 (1,502) | EU10126 (89.7; 1,470), sulfidic cave stream biofilm |
| G | 16,786 | 47.5 | c_Alphaproteobacteria, o_Rhodospirillales uncultured metagenome (MAG from soil), FPLS01028346.18.1488 (80.9; 1,474) | MZ229987 (1,482) | AB494774 (81.8; 1503), artificial mesocosm enriched with sheep rumen fluid |
| W ^f | 2,336 | 7.3 | | MZ229992 (1,482) | |

^aThe fifth column lists NCBI GenBank accession numbers of sequences assembled in this study, where identical sequences from library G and W are indicated by asterisks (*). The last column summarizes the BLAST results of all assembled sequences.

^bSILVA NR97 best hit from phyloFlash, values before the first period are searchable in SILVA and GenBank.

^cGenBank best hit accessed 1/10/22.

^dOnly SILVA entry to return a Genome Taxonomy Database (GTDB) taxonomy besides “unclassified”: d_Bacteria; p_Desulfobacterota; c_Desulfobacteria; o_Desulfobacterales; f_BuS5; g_BuS5; s_BuS5 sp000472805.

^eSequence also found in MAG W9 (see Table 2).

^fSequence was also found in MAG W7 (see Table 2).

Sulfurospirillum (average % identity = 97.3%, Data Set S5). The predominance was remarkable, with >61% of bacterial reads assigned to the genus *Sulfurospirillum* and 91% assigned to the order *Campylobacterales* ($n = 346,877$ reads, Data Set S5). Analysis by SingleM (Table S2) also showed a predominance of reads assigned to *Sulfurospirillaceae*, with up to 88% of reads from Library G assigned to this family. The next most abundant classification across all markers was unassigned (Table 4). SAR324 was again identified only in Library W (Data Set S6), see Supplemental File 1 for additional information.

(i) Methanotrophic, methylotrophic, and archaeal taxonomic assignments. Few reads affiliated with aerobic or anaerobic methanotrophic/methylotrophic taxa were recovered. Most assignments were to families and genera from the order *Methylococcales*, with 113 reads mapped to SILVA (12) (Data Set S3) and 573 reads mapped to the manually curated 16S rRNA database focused on methane hydrate and seep studies (Data Set S5). Although *Methylococcales* 16S rRNA gene signatures were identified in the metagenomes, few reads matched particulate methane monooxygenase (*pmoA*) sequences ($n = 14$ reads). Furthermore, annotations were generally poor based on the number of identical best hits provided by mated paired-end reads ($n = 2$, Table S6). Low competitive

TABLE 2 Metagenome-assembled genomes (MAGs) produced from *S. methanicola* gut contents (G) and worm fragment (W) libraries separately assembled using MEGAHIT and binned using MetaBat2, MaxBin2, DAS Tool, and Anvi'o^a

| MAG name | NCBI genome accession no. (this study) | Predicted taxonomy (GTDB) | Total length (mbp) | No. contigs | Completeness | | Redundancy Anvi'o |
|------------|--|---|--------------------|-------------|--------------|--------|-------------------|
| | | | | | CheckM | Anvi'o | |
| W8 | JAERRW0000000000 | <i>o_Campylobacteriales; f_Sulfurospirillaceae; g_Sulfurospirillum</i> | 1.51 | 106 | 97.18 | 94.37 | 1.41 |
| G15 | JAERRY0000000000 | | 1.66 | 145 | 95.26 | 97.18 | 2.82 |
| G18 | JAERRX0000000000 | <i>o_Campylobacteriales; f_Thiovulaceae; g_Sulfurimonas</i> | 1.92 | 190 | 86.53 | 97.18 | 1.41 |
| W9 | JAERRU0000000000 | <i>o_SAR324</i> | 1.52 | 42 | 87.79 | 94.37 | 0 |
| G10 | JAERRP0000000000 | <i>o_Desulfobacteriales; f_UBA5852</i> | 4.42 | 925 | 86.73 | 84.51 | 7.04 |
| G11 | JAERRQ0000000000 | <i>o_Desulfobacteriales; f_Bu55</i> | 2.2 | 411 | 83.23 | 87.32 | 4.23 |
| W7 | JAERRO0000000000 | <i>c_Alphaproteobacteria; o_Rs-D84</i> | 0.67 | 23 | 78.57 | 87.32 | 0 |
| G3 | JAERM0000000000 | | 0.64 | 32 | 78.57 | 87.32 | 0 |
| G12 | JAERRZ0000000000 | <i>o_Enterobacteriales; f_Alteromonadaceae; g_Colwellia</i> | 2.71 | 660 | 76.06 | 90.14 | 4.23 |
| G4 | JAERRN0000000000 | <i>c_Alphaproteobacteria; o_Rickettsiales; g_UBA4311</i> | 0.96 | 81 | 74.39 | 88.73 | 0 |
| G13 | JAERSA0000000000 | <i>o_Enterobacteriales; f_Alteromonadaceae; g_Pseudoalteromonas; s_undina</i> | 2.34 | 576 | 68.75 | 80.28 | 0 |
| G19_1 | JAERSO0000000000 | <i>o_Desulfobacteriales; f_Bu55</i> | 1.49 | 309 | 67.82 | 50.7 | 9.86 |
| G19_2 | JAERTT0000000000 | | 1.16 | 347 | 31.33 | 49.3 | 2.82 |
| G20 | JAERRY0000000000 | <i>o_Campylobacteriales; f_Sulfurovaceae; g_SZUA-451</i> | 1.12 | 306 | 64.86 | 71.83 | 4.23 |
| W6 | JAERSB0000000000 | <i>o_Mycoplasmatales; f_UBA3375</i> | 0.34 | 100 | 52.55 | 60.56 | 0 |
| G16 | JAERRR0000000000 | <i>o_Desulfobacteriales; f_Bu55</i> | 0.48 | 129 | 11.61 | 43.66 | 0 |

^aNearly identical MAGs are indicated in bold. Anvi'o refinement resulted in MAG G19 being split because coverage-based hierarchical clustering of the contigs produced two distinct clusters. Additional quality and read recruitment data are provided in Table S4. GTDB = Genome Taxonomy Database.

Phylogenomic tree

Tree scale: 1

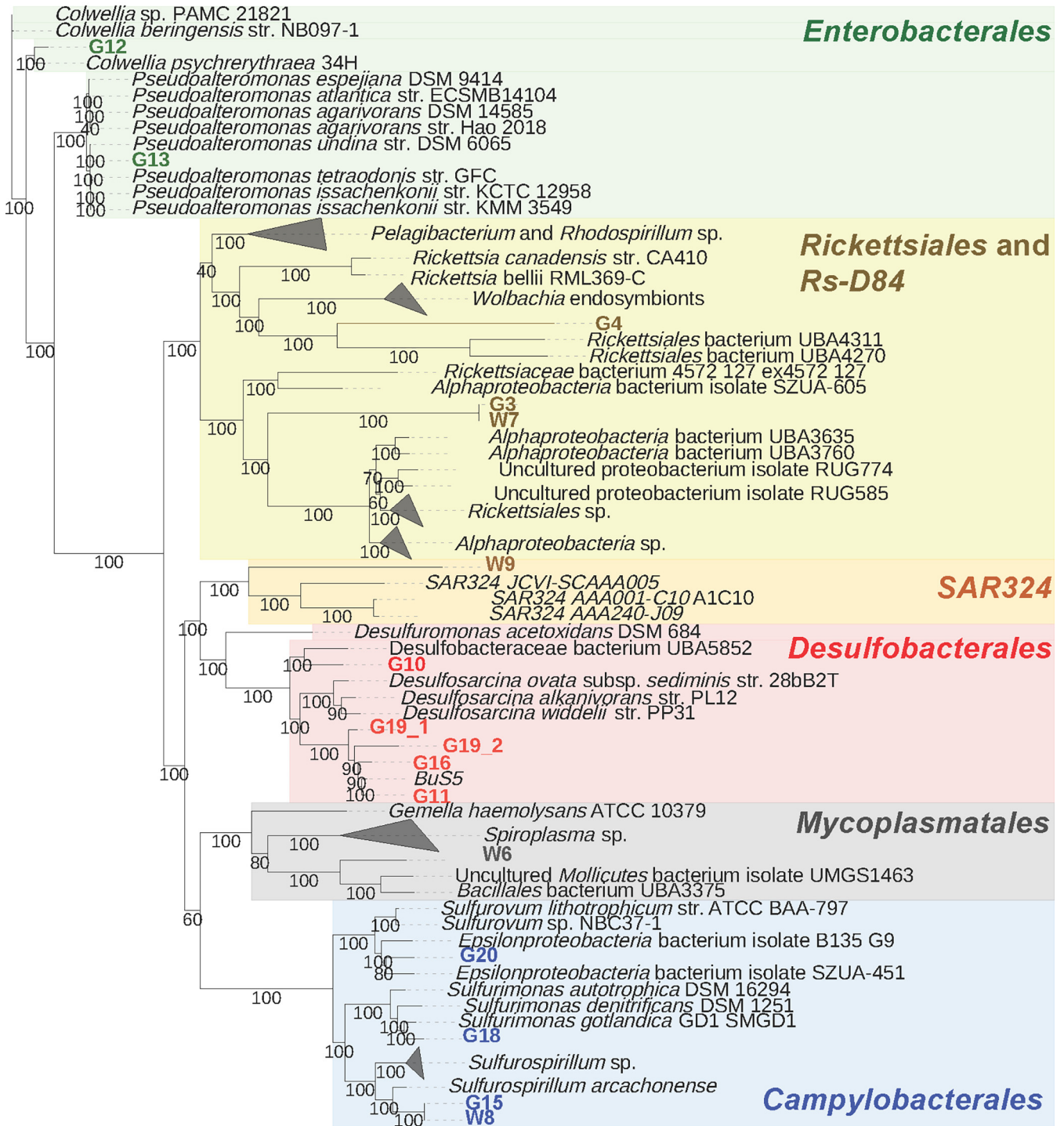


FIG 3 Phylogenomic tree of prokaryotes associated with metagenome-assembled genomes (MAGs) recovered from HiSeq libraries generated from *S. methanicola* gut contents (G) and worm fragments (W). The tree is unrooted and based on the concatenated amino acid sequence alignment (17,533 aa) of 71 marker genes identified by anvio. Bootstrap values, based on 100 replicates, are indicated on the nodes. The scale bar indicates 1 substitution per site. NCBI accession numbers for MAGs are listed in Table 2.

TABLE 3 Bacterial taxonomic classifications to family (top 11) assigned to two *S. methanicola* metagenomes (sum from Library G and W, HiSeq) based on phyloFlash extraction of partial 16S rRNA gene sequences mapped to SILVA (Data Set S3) and Magic-BLAST mapping to Data Set S4 containing 16S rRNA sequences of uncultivated taxa from methane hydrate and cold seep studies (Data Set S5, includes % identities)

| Family, PhyloFlash-SILVA | Sum of Read Count | % | Family, Magic-Blast-Data Set S4 | Sum of Read Count | % |
|--------------------------------------|-------------------|-----|---|-------------------|------|
| <i>Sulfurospirillaceae</i> | 300980 | 64 | <i>Sulfurospirillaceae</i> | 210433 | 61 |
| Unassigned to family | 108478 | 23 | <i>Sulfurimonadaceae</i> | 45822 | 13 |
| <i>Sulfurovaceae</i> | 10711 | 2 | <i>Arcobacteraceae</i> | 35394 | 10 |
| <i>Sulfurimonadaceae</i> | 5939 | 1.3 | <i>Sulfurovaceae</i> | 21485 | 6 |
| <i>Bacillaceae</i> | 5442 | 1.2 | <i>Desulfatiglandaceae</i> | 7610 | 2 |
| <i>Enterobacteriaceae</i> | 4841 | 1.0 | <i>Entomoplasmatales Incertae Sedis</i> | 4602 | 1.3 |
| <i>Campylobacteraceae</i> | 3638 | 0.8 | <i>Fusibacteraceae</i> | 4484 | 1.3 |
| <i>Arcobacteraceae</i> | 3504 | 0.7 | <i>Desulfosarcinaceae</i> | 4032 | 1.2 |
| <i>Mycoplasmataceae</i> ^a | 3313 | 0.7 | <i>Campylobacteraceae</i> | 3003 | 0.9 |
| <i>Legionellaceae</i> ^a | 2467 | 0.5 | <i>Bacteroidetes_BD2-2</i> | 2042 | 0.6 |
| <i>Desulfosarcinaceae</i> | 2057 | 0.4 | <i>Methylomonadaceae</i> ^d | 573 | 0.17 |
| Total | 471,640 | | Total | 346,877 | |

^aNot represented in Data Set S4.

read recruitment was observed in 22 published MAGs associated with methane hydrates (13) (0.07% of Library G mapped reads; 0.05% of Library W mapped reads). Reads predominantly recruited to the *S. methanicola*-associated MAGs described here (>99% of mapped reads from both libraries) (Data Set S2).

Querying against methyl coenzyme M reductase (*mcrA*) from uncultured methanogenic archaea (Data Set S4) recovered 10 reads (5 mate-pairs) classified as ANME-1, ANME-2, or ANME-2a, all with identical annotations for mated read pairs and most with 100% identity to reference sequences (Table S7). Read recruitment was negligible (0.0001% of mapped reads from library G; 0.001% of mapped reads from library W) to 36 MAGs associated with freshwater ANME-2d (14) (Data Set S2).

Overall, few reads were identified as archaeal. Only 28 reads mapped to archaeal 16S rRNA gene sequences in SILVA (Data Set S3). Few archaeal reads were identified by single-copy marker genes (*n* = 11, Data Set S6). Of the 64 reads identified in the manually curated database (Data Set S4), 78% were assigned to *Woesearchaeales* (Data Set S5). See Supplemental File 1 for additional details.

MAG functional profiles. Functional analysis revealed a range of metabolic capacities in the microbiomes analyzed here. Predicted electron acceptors included oxygen (see Supplemental File 1 for details), nitrate, nitrite, sulfate, sulfide, thiosulfate, tetrathionate, fumarate, and possibly dimethyl sulfoxide (DMSO) (Fig. 4). Denitrification (Fig. S1), nitrogen fixation (Fig. S2), anaerobic alkane oxidation (Fig. S3A), and aromatic compound degradation (Fig. S3B) genes were identified in some MAGs. Predicted central carbon metabolic pathways included the pentose phosphate pathway (PPP), gluconeogenesis, fatty acid oxidation, glycolysis, carbohydrate degradation, tricarboxylic acid (TCA) cycle, and acetate

TABLE 4 Bacterial taxonomic classifications (Data Set S6) for assignments across all SingleM marker genes (Table S2) for reads >1% in either metagenomic library

| Taxonomic assignment | No. reads, library G | % | No. reads, library W | % |
|----------------------------|----------------------|-----|----------------------|-----|
| <i>Sulfurospirillaceae</i> | 26657 | 61 | 760 | 42 |
| Unassigned | 4681 | 11 | 521 | 29 |
| <i>Campylobacteraceae</i> | 4064 | 9 | 113 | 6 |
| <i>Thiovulaceae</i> | 3203 | 7 | 80 | 4 |
| <i>Nautiliaceae</i> | 1758 | 4 | 47 | 3 |
| <i>Rickettsiaceae</i> | 538 | 1 | 66 | 4 |
| <i>Sulfurovaceae</i> | 479 | 1 | 9 | 0.5 |
| <i>Enterobacteriaceae</i> | 288 | 0.7 | 47 | 3 |
| <i>Corynebacteriaceae</i> | 215 | 0.5 | 21 | 1 |
| <i>Mycoplasmataceae</i> | 174 | 0.4 | 4 | 0.2 |
| <i>Acholeplasmataceae</i> | 165 | 0.4 | 19 | 1 |
| Total | 43709 | | 521 | |

Electron accepting reactions in *S. methanicola*'s microbiome

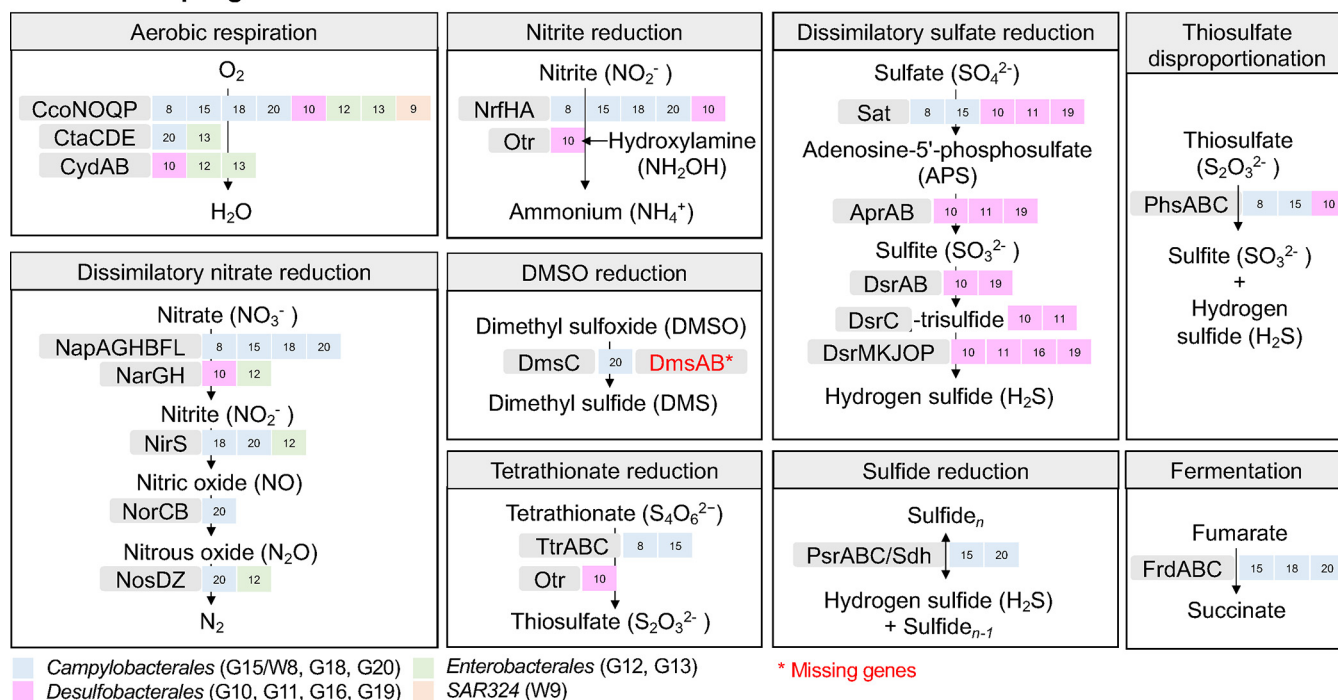


FIG 4 Overview of electron-accepting reactions in MAGs generated for *S. methanicola*. Colored boxes indicate the MAG number(s) where each gene was detected. Missing genes are denoted in red text. Abbreviations are listed in Table S8.

conversions (Fig. 5). Acetogenesis was predicted for all the *Campylobacteriales*, *Desulfobacteriales*, and *Enterobacteriales* MAGs except for G13 (Data Set S7). Details on gene annotations are in Data Set S7 and gene name abbreviations are in Table S8.

(i) Sulfur reducers. *Sulfurospirillum* (order *Campylobacteriales*) was assigned to the predominant MAGs, G15, and W8. The ability to reduce nitrate, nitrite, and a range of sulfur compounds was predicted (Fig. 4, Data Set S7). The automated annotation software METABOLIC (Table S2) only detected the *phsA* gene for thiosulfate disproportionation. However, 12 additional sulfur pathway genes were detected through automated and manual curation (Table S2, Fig. S1, and Data Set S7). These included genes catalyzing tetrathionate reduction and bidirectional polysulfide reduction/sulfide oxidation, as reported in *Sulfurospirillum multivorans* (13) and uncultured *Sulfurospirillum cavolei* MES (14). Although the genetic capacity to activate sulfate in the dissimilatory sulfate reduction pathway via sulfate adenytransferase (*sat*) was observed, a complete pathway was not detected. These MAGs also predicted the ability to use fumarate as an electron acceptor during fermentation to produce succinate (Fig. 4). The functional capacities to reduce halogenated compounds, arsenate, selenate, or nitrous oxide were not detected in these MAGs.

(ii) Sulfate reducers. The ability to reduce sulfate and sulfite was predicted by a suite of dissimilatory sulfate reduction genes present in all MAGs assigned to the order *Desulfobacteriales* (G10, G11, G16, and G19) (Fig. 4, Fig. S1, and Data Set S7). Overall, these MAGs indicated the genetic potential to couple exergonic sulfate reduction to endergonic acetate oxidation through the reverse Wood-Ljungdahl pathway (Fig. 5, Fig. S4, and Data Set S7), in which CO, tetrahydrofolate-linked intermediates (5-methyl-tetrahydrofolate, methylene-tetrahydrofolate, methenyl-tetrahydrofolate, and formyl-tetrahydrofolate), and formate could be oxidized into CO₂. All MAGs classified as *Desulfobacteriales* also contained the sulfur dioxygenase (*sdo*) gene catalyzing glutathione-dependent sulfide oxidation (Fig. S1 and Data Set S7).

Members of this group were predicted to reduce arsenate via arsenate reductases, oxidize hydrogen for energy via [Ni-Fe] hydrogenase (Fig. S1 and Data Set S7), and

Predicted prokaryotic carbon cycling pathways in *S. methanicola*

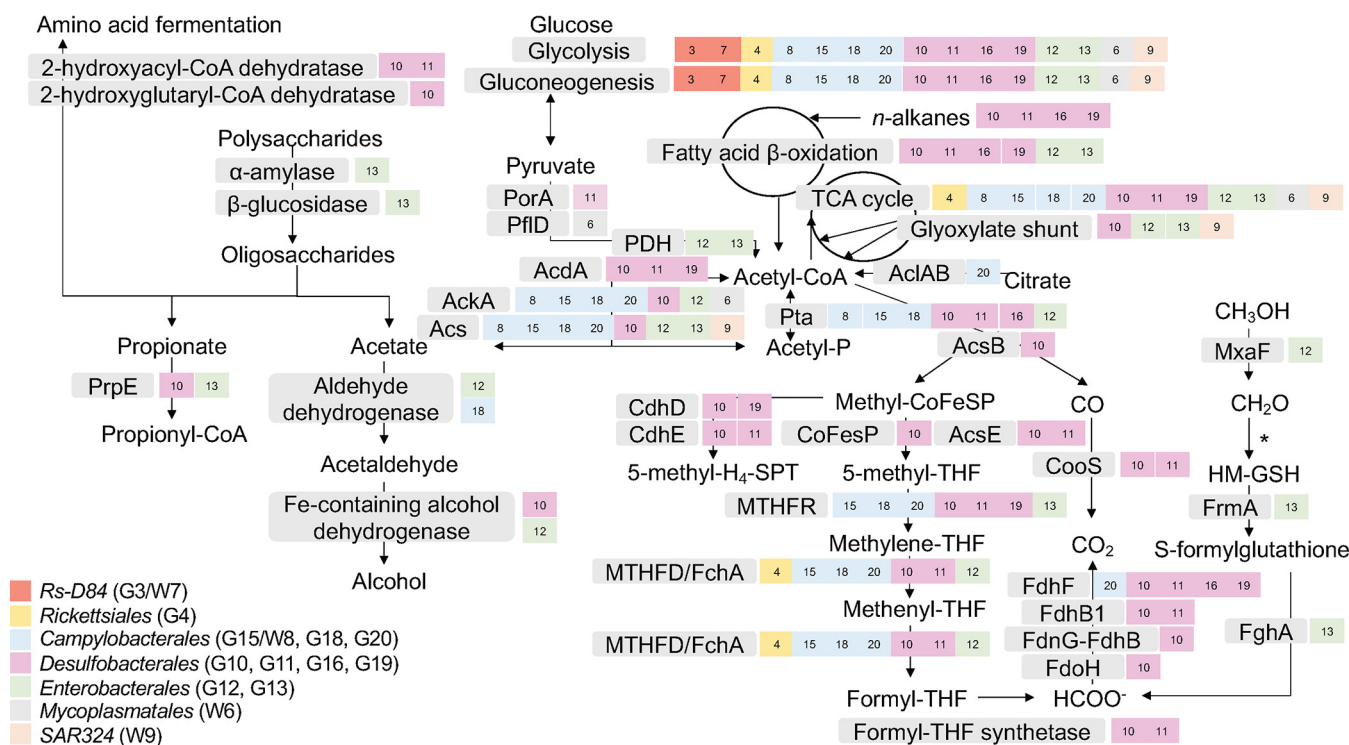


FIG 5 Overview of carbon metabolism pathways identified in MAGs generated for *S. methanicola*. Colored boxes indicate MAG number(s) where each gene or pathway is detected. Spontaneous reactions are indicated by asterisks (*). Abbreviations are listed in Table S8.

carry out anaerobic alkane oxidation via alkylsuccinate synthase (Fig. S3A). Nitrogen fixation genes were detected, including *nifAHDKB* in MAG G10, *nifH* in MAG G11, and *nifHENB* in MAG G19. In addition, genes encoding the P-II family nitrogen regulator, [2Fe-2S] ferredoxin, and GCN5-related-N-acetyltransferase were detected based on homology to the *nif* operon of *Desulfatibacillum aliphaticivorans* (Fig. S2). Additional pathways predicted in these MAGs are detailed in Supplemental File 1.

(iii) Nitrate-reducing, sulfur-oxidizing bacteria. The ability to reduce nitrate and oxidize sulfur under aerobic/microaerophilic conditions was predicted for MAG G18 classified as *Sulfurimonas* and for MAG G20 classified as *Sulfurovaceae SZUA-451*. Overall, predicted potential electron donors for this group included sulfur compounds, hydrogen, and certain methylotrophic compounds. Potential electron acceptors included oxygen, nitrogenous compounds, fumarate, and perhaps DMSO (Fig. 4 and 5, Fig. S1 and S4, and Data Set S7). Nitrate respiration through dissimilatory nitrate reduction to ammonium (15) was predicted for both MAG G18 and G20 (*napABFGHL* and *nrfA*). Denitrification was predicted for MAG G20 (*nirS*, *norBC*, and *nosDZ*) (Fig. S1 and Data Set S7). Thiosulfate oxidation to provide metabolic energy (*soxCD* and *soxYZ*) was predicted for both MAGs. Some genes associated with nitrate reduction/sulfur oxidation also were detected in G12 classified as *Colwellia* (see Supplemental File 1 for details).

The ability to degrade benzoate, toluene, xylene, and phenol was predicted for G18 classified as *Sulfurimonas* with 41× mean coverage of aromatic compound degradation gene clusters. In addition, genes encoding aromatic compound degradation were detected in an unbinned contig (not belonging to a MAG) assigned to *Arcobacter* with 67× mean coverage, and an unbinned proteobacterial contig with 38× mean coverage (Fig. S3B and Supplemental File 1).

(iv) Enteric bacteria. Genes indicative of assimilatory sulfate reduction (*cysND*) were predicted in MAGs assigned to the order *Enterobacteriales*, including G12 classified as *Colwellia* spp. and G13 classified as *Pseudoalteromonas undina* (Fig. S1 and Data Set S7).

Some genes found in nitrate-reducing, sulfur-oxidizing bacteria were detected in G12 (see Supplemental File 1 for details). Genes were detected for the oxidation of methanol in G12 (*mxoF*), and formaldehyde in G13 (*frmA* and *fghA*), but C1 pathways were incomplete (Fig. 5, Fig. S4, and Data Set S7). Autotrophic genes were not detected in these MAGs.

(v) Other microbial taxa. MAGs classified as *SAR324*, *Alphaproteobacteria*, and *Mycoplasmatales* are detailed in Supplemental File 1.

(vi) B vitamin biosynthesis. Microbial biosynthesis of vitamins B1, B2, B3, B5, B6, B7, and B9 were predicted in MAGs classified as *Campylobacteriales*, *Desulfobacteriales*, and *Enterobacteriales*. Except for vitamin B7, biosynthesis of these vitamins also was predicted for MAG W9 classified as *SAR324* (Data Set S8). A partial vitamin B12 biosynthesis pathway was identified in MAG G11 classified as *Desulfobacteriales* *BuS5*, G12 classified as *Colwellia*, G18 classified as *Sulfurimonas*, and G20 classified as *Sulfurovaceae* *SZUA-451* (Table S9 and Data Set S8).

(vii) Amino acid biosynthesis. Amino acid biosynthesis pathways were annotated in all MAGs with various completeness, except G3/W7 (classified as *Alphaproteobacteria* *Rs-D84*) in which no amino acid biosynthesis pathway was predicted (Table S9). The abundant MAGs classified as *Sulfurospirillum* (G15 and W8) contained biosynthetic genes for all 20 essential amino acids (Table S9 and Data Set S8). Histidine and lysine biosynthesis pathways were not in any of the MAGs assigned to order *Desulfobacteriales*. MAGs assigned to order *Enterobacteriales* (G12 and G13) contained chorismate synthesis genes, but not genes in downstream aromatic amino acids biosynthesis pathways. Homocysteine and methionine biosynthetic pathways were not detected in G13, while biosynthetic pathways for branched-chain amino acids were not detected in G12 (Table S9 and Data Set S8).

DISCUSSION

Paired taxonomic and functional profiles were obtained for microbiomes associated with the methane ice worm. Metabolic pathways featured a variety of nitrogen (Fig. 4), organic carbon (Fig. 5), and sulfur (Data Set S7) compounds. Thiosulfate disproportionation, nitrite ammonification, fumarate fermentation, and the reduction of nitrate, tetrathionate, and sulfide (Fig. 4) were predicted to be key processes, based on the predominance of sequences assigned to uncultured *Sulfurospirillum* in the *S. methanicola* metagenomes (Table 1 to 4). *Sulfurospirillum* spp. specialize in degrading fermentation products coupled to anaerobic respiration of a wide variety of terminal electron acceptors, including sulfur and nitrogen compounds with intermediate valence states (14, 16), such as thiosulfate (Fig. 4).

The microbial diversity of *S. methanicola* metagenomes described here was distinct from taxonomic profiles described for methane hydrates in the literature (5, 7, 11, 17, 18). Chemoautotrophic sulfur-oxidizing bacteria are thought to be a primary food source for the worms (2, 3), and DNA clones obtained from Gulf Mexico gas hydrates did not reveal numerically dominant taxa (5). In contrast, the worm metagenomes described here were predominated by a single taxon classified as *Sulfurospirillum* (Table 1 to 4). Furthermore, weak recruitment of reads was observed to environmental MAGs available in the literature. Instead, almost all reads recruited to the MAGs recovered from *S. methanicola* (Data Set S2). Overall, this line of reasoning suggested that phylogenetic relatives of *Sulfurospirillum* represent members of the core microbiome or “normal symbiotic state” (19) of this marine polychaete. This is a noteworthy finding because *Sulfurospirillum* is categorized as free-living in the literature (20, 21).

The worms were collected from oil-rich areas and environmental exposure to hydrocarbons was indicated by a petroleum smell emanating from the worm gut when pierced during dissection (Table S1). The mechanisms employed by the worm to manage chemical exposure, including the role of the microbiome, are currently unknown. The ability to utilize alkanes, benzoate, toluene, xylene, and phenol was predicted in these metagenomes (Fig. S3). In addition, evidence of arsenic resistance was detected in multiple MAGs classified as *Desulfobacteriales*, *Sulfurimonas*, *Sulfurovaceae*, and *Colwellia*, as detailed in Supplemental File 1. A number of the taxa identified here

are known to degrade toxic compounds. For example, *Sulfurospirillum* is often the dominant species in oil-contaminated samples (21) and some can respire organohalides (22). *Desulfobacterales*, *Sulfurimonas*, and *Colwellia* have been shown to degrade hydrocarbons in marine systems (23–25).

Furthermore, sulfur cycling may expose *S. methanicola* to toxic intermediates. Black particulates of unknown composition were noted in the gut contents (Table S1), which likely contained sulfur based on predicted metabolic pathways (Fig. 4). All MAGs classified as *Desulfobacterales* contained the sulfur dioxygenase (*sdo*) gene (see Supplemental File 1 for details). This gene is generally considered part of H₂S detoxification in animals, although generation of adenosine triphosphate (ATP) can occur (26). Black granular particulates and amorphous organic material were similarly observed in the stomachs and, to a smaller extent, midgut of *Rimicaris exoculata* juveniles (hydrothermal vent shrimp) (27). This material was believed to be a nutrition source for these juveniles before they switch to a mainly epibiont-based diet in their adult forms (27).

The presence of prokaryotic biosynthetic genes for B vitamins and amino acids (Table S9 and Data Set S8) in these metagenomes suggested that bacteria may provide a source of these substances to the host, *S. methanicola*. Soluble B vitamins, including vitamins B1, B7, and B12, are limited in availability and ecologically important in marine habitats (28). In the polychaete *Capitella teleta*, vitamins B2 and B3 were crucial for larval metamorphosis (29), and vitamin B12 provided by bacteria is hypothesized to be critical to worm health (30). Similarly, the SAR324 major syncytial tissue symbiont in the glass sponge *Vazella pourtalesii* was hypothesized to provide amino acids and B vitamins to other microbial symbionts and the host (31).

Few ANME, methanotrophic, or methylotrophic signatures were observed in these metagenomes (Table S6 and S7 and Data Set S4 and S7). ANME taxa are key features at methane seeps (8), but worm bioerosion may be incompatible with ANME's strict anaerobic requirements (32). Methanotrophs appear to be the primary food source for ampharetid polychaetes living at methane seeps in New Zealand (33). However, this is not the case for *S. methanicola* living on Gulf of Mexico methane hydrates according to stable isotope measurements (3). Although we were unable to determine worm food sources in this study, prey species likely take advantage of compounds that provide more metabolic energy than methane. Gas hydrates can be rich in H₂S, hydrocarbons, ethane, propane, iso-butane, butane, and pentane (2, 7, 11). Furthermore, rates of anaerobic methane oxidation in the Gulf of Mexico are at least 2 orders of magnitude lower than sulfate reduction rates (7).

These samples were analyzed for RNA, protein, and long-read DNA sequences to extend the MAG analysis here, but the data quality was unsatisfactory. Therefore, future sampling and, if possible, culture isolation and feeding experiments are needed to provide robust functional inferences. However, *S. methanicola* is difficult to obtain. We attempted to collect more samples from GC234 in June 2021 but only small methane hydrates devoid of *S. methanicola* were observed. Therefore, the data sets provided in this report (Data Set S2 to S8) provide a rare opportunity for further metagenomic mining. For example, sequences were assigned to almost 200 bacterial families (Data Set S3), although the main text reviews only about 10 of the most dominant families (Table S3).

The *S. methanicola* microbiome contained both sulfur oxidation and reduction pathways, suggesting syntrophic microbial sulfur cycling. Such pathways are known in marine sediments and animal symbionts (34–36). From the perspective of comparative biology, *S. methanicola* provides an organism of interest given that dysbiosis is associated with sulfur compound cycling in the human gut (37). Gut microbiomes are known to cluster with host diet (38) and trophic levels (39). It thus follows that although the life history of the methane ice worm is novel, its microbiome could provide insight into the biology of other deep-sea species. Notably, high abundances of *Sulfurospirillum* were reported in the gut of the hydrothermal vent crab *Austinograea* sp. (40), which is also known to feed on bacteria (41). Overall, these data encourage further studies to

confirm the metabolism and feeding behavior of *S. methanicola*, roles of gut bacteria, and species interactions within this unconventional ecosystem.

MATERIALS AND METHODS

Sample collection and processing. Live *S. methanicola* was collected from a methane hydrate located at a depth of 542.8 m in the Green Canyon area (GC234) of the Gulf of Mexico (27°44.7526' N, 91°13.3168' W) (Fig. 1). Specimens were retrieved using the manipulator arm of the crewed *Johnson Sea-Link II* submersible during Dive number 3751 (October 3, 2009, 10:31 am UTC, operated by Harbor Branch Oceanographic Institute, Fort Pierce, FL, USA) and brought on board the R/V Seward Johnson during cruise SJ-2009-GOM. Worms were rinsed with 0.2- μ m filtered seawater before aseptic dissection to expose the worm gut but were otherwise untreated with antiseptics and antibiotics and therefore not considered axenic. Gut contents were extracted with a sterile syringe and worm fragments left over from the dissection were also saved (Fig. 2 and Table S1), with details provided in Supplemental File 1. The method of dissection was such that the two libraries were not expected to be strictly constrained to "gut" or "non-gut" sequences (e.g., the worm fragment library likely contained gut tissues). All samples were stored at -80°C until DNA extraction and library preparation, as described in Supplemental File 1. Subsequent attempts to obtain more specimens, most recently in June 2021, were not successful.

Read-based taxonomic classification. Reads from the HiSeq shotgun metagenomic libraries (Table S1) were analyzed by a variety of bioinformatics tools (Table S2). Briefly, reads from each library were assembled separately using the default parameters of SPAdes implemented in phyloFlash v3.4 (42) with the taxonomy of the extracted full-length small subunit (SSU) rRNA sequences checked by NCBI megablast. Reads that failed to assemble were subsequently mapped to SILVA (12) as part of the phyloFlash pipeline (Data Set S3). Reads also were mapped to 14 single-copy marker genes using SingleM v0.13.2 (Data Set S6). Three custom databases were built from *pmoA*, *mcrA*, or 16S rRNA sequences of uncultured taxa from methane hydrate and seep studies, with annotation for 16S rRNA sequences enhanced by QIIME2 analysis (Data Set S4). Magic-BLAST v1.5.0 (Table S2) was used to map paired-end reads to these mapping databases (Data Set S5).

Metagenomic assembly and characterization. Metagenomic assembly, binning, taxonomic classification, and read recruitment methods are detailed in Supplemental File 1. Briefly, each metagenomic library was individually assembled using MEGAHIT (43) and quality-checked with *anvi'o* (44) and CheckM (45). MAGs were taxonomically classified using the Genome Taxonomy Database toolkit GTDB-tk (46) and a phylogenomic tree was constructed with genomes downloaded from NCBI. MAG pairwise amino acid identities (AAIs) were calculated using CompareM. Read recruitment was estimated by mapping against MAG databases built from (i) this study, (ii) methane hydrate sediments (17), (iii) freshwater *Methanoperedens* (methane-oxidizing archaea) and associated extrachromosomal elements (47), and (iv) a concatenation of these three sets of sequences (Data Set S2).

(i) MAG functional annotation. As detailed in Table S2, metagenomes were annotated with a variety of tools, including METABOLIC v4.0 (48), *anvi'o* (44), and the classicRAST annotation scheme (49), with annotations verified using web BLAST (50) searches against the NCBI nonredundant protein and nucleotide (nr/nt) databases (51). Manual annotation was also used to identify metabolic genes in *S. methanicola*-associated MAGs. Reference protein sequences curated from uncultured and cultured *Sulfurospirillum* genomes (14) and those from the alkylsuccinate synthase clusters in *Desulfatibacillum aliphaticivorans* AK-01 (52) were queried against protein sequences predicted from *S. methanicola*-associated MAGs using local BLASTp searches with a percentage identity cutoff of 30% and E value cutoff of 1×10^{-6} . Other genes involved in the "Aromatics degradation" KEGG pathway module were identified using ghostKOALA (Table S2) and their annotations were similarly verified using web BLAST (50) searches. RAST was used to identify the *Desulfatibacillum aliphaticivorans* AK-01 (52) genome relative (NCBI accession number [NC_011768](#)) of *nif* gene clusters and their corresponding positions in *S. methanicola*-associated MAGs (Fig. S2). Pathways and gene functions were curated using the MetaCyc metabolic pathway database (53).

Data availability. Sequenced reads, full-length SSU sequences, metagenomes, and MAG assemblies were deposited in NCBI under the BioProject ID [PRJNA689840](#).

SUPPLEMENTAL MATERIAL

Supplemental material is available online only.

SUPPLEMENTAL FILE 1, PDF file, 1.2 MB.

SUPPLEMENTAL FILE 2, XLSX file, 0.04 MB.

SUPPLEMENTAL FILE 3, XLSX file, 0.3 MB.

SUPPLEMENTAL FILE 4, XLSX file, 0.6 MB.

SUPPLEMENTAL FILE 5, XLSX file, 44 MB.

SUPPLEMENTAL FILE 6, XLSX file, 2.4 MB.

SUPPLEMENTAL FILE 7, XLSX file, 0.1 MB.

SUPPLEMENTAL FILE 8, XLSX file, 0.02 MB.

ACKNOWLEDGMENTS

This research was carried out [in part] under the auspices of the Cooperative Institute for Marine and Atmospheric Studies (CIMAS), a Cooperative Institute of the University of Miami, and the National Oceanic and Atmospheric Administration, cooperative agreement number NA200AR4320472, with support from the NOAA Office of Oceanic and Atmospheric Research's 'Omics Initiative. This work was supported by award NA16OAR4320199 to the Northern Gulf Institute from NOAA's Office of Oceanic and Atmospheric Research, U.S. Department of Commerce. Sample collection was supported in part by NSF OCE-0527139. NIH grant 1R21-ES024105 supported preliminary computational analysis. MiSeq sequencing was performed through NSF DUE-1323809, which supported a Sequencing Technology Education using Microbial Metagenomes (STEMM) workshop at San Diego State University organized by Elizabeth Dinsdale.

Early data analysis efforts were undertaken by Wei Xin of Smith College and Lee Edsall and Nick Smith of the University of California, San Diego (UCSD). Richard Emlet, University of Oregon, is gratefully acknowledged for the skilled dissection that provided the Tube A sample. We gratefully acknowledge the nucleic acid processing and HiSeq2000 sequencing efforts of Steve Head and Terry Gelbart at the Scripps Research Institute. We thank Michelle Wood (Co-PI on NSF OCE-0527139) for inviting KG on the cruise and for promoting metagenomic research, including this methane ice worm study. We thank Barbara Campbell, Nastassia Patin, and Michelle Wood for helpful reviews of the draft manuscript.

We declare no conflict of interest.

REFERENCES

- Desbruyères D, Toulmond A. 1998. A new species of hesionid worm, *Hesiocaeca methanicola* sp. nov. (Polychaeta: Hesionidae), living in ice-like methane hydrates in the deep Gulf of Mexico. *Cah Biol Mar* 39:93–98.
- Fisher CR, MacDonald IR, Sassen R, Young CM, Macko SA, Hourdez S, Carney RS, Joye S, McMullin E. 2000. Methane ice worms: *Hesiocaeca methanicola* colonizing fossil fuel reserves. *Naturwissenschaften* 87:184–187. <https://doi.org/10.1007/s001140050700>.
- Becker EL, Cordes EE, Macko SA, Lee RW, Fisher CR. 2013. Using stable isotope compositions of animal tissues to infer trophic interactions in Gulf of Mexico lower slope seep communities. *PLoS One* 8:e74459. <https://doi.org/10.1371/journal.pone.0074459>.
- Pile AJ, Young CM. 2006. Consumption of bacteria by larvae of a deep-sea polychaete. *Marine Ecology* 27:15–19. <https://doi.org/10.1111/j.1439-0485.2006.00084.x>.
- Mills HJ, Martinez RJ, Story S, Sobecky PA. 2005. Characterization of microbial community structure in Gulf of Mexico gas hydrates: comparative analysis of DNA- and RNA-derived clone libraries. *Appl Environ Microbiol* 71:3235–3247. <https://doi.org/10.1128/AEM.71.6.3235-3247.2005>.
- Lanoil BD, Sassen R, La Duc MT, Sweet ST, Nealson KH. 2001. Bacteria and archaea physically associated with Gulf of Mexico gas hydrates. *Appl Environ Microbiol* 67:5143–5153. <https://doi.org/10.1128/AEM.67.11.5143-5153.2001>.
- Orcutt BN, Boetius A, Lugo SK, MacDonald IR, Samarkin VA, Joye SB. 2004. Life at the edge of methane ice: microbial cycling of carbon and sulfur in Gulf of Mexico gas hydrates. *Chem Geol* 205:239–251. <https://doi.org/10.1016/j.chemgeo.2003.12.020>.
- Mills HJ, Hodges C, Wilson K, MacDonald IR, Sobecky PA. 2003. Microbial diversity in sediments associated with surface-breaching gas hydrate mounds in the Gulf of Mexico. *FEMS Microbiol Ecol* 46:39–52. [https://doi.org/10.1016/S0168-6496\(03\)00191-0](https://doi.org/10.1016/S0168-6496(03)00191-0).
- Waite DW, Chuvochina M, Pelikan C, Parks DH, Yilmaz P, Wagner M, Loy A, Naganuma T, Nakai R, Whitman WB, Hahn MW, Kuever J, Hugenholtz P. 2020. Proposal to reclassify the proteobacterial classes Deltaproteobacteria and Oligoflexia, and the phylum Thermodesulfobacteria into four phyla reflecting major functional capabilities. *Int J Syst Evol Microbiol* 70: 5972–6016. <https://doi.org/10.1099/ijsem.0.004213>.
- Waite DW, Vanwonterghem I, Rinke C, Parks DH, Zhang Y, Takai K, Sievert SM, Simon J, Campbell BJ, Hanson TE, Woyke T, Klotz MG, Hugenholtz P. 2018. Addendum: comparative genomic analysis of the class Epsilonproteobacteria and proposed reclassification to Epsilonbacteraeota (phyl. nov.). *Front Microbiol* 9:772. <https://doi.org/10.3389/fmicb.2018.00772>.
- Kvenvolden KA. 1995. A review of the geochemistry of methane in natural gas hydrate. *Organic Geochemistry* 23:997–1008. [https://doi.org/10.1016/0146-6380\(96\)00002-2](https://doi.org/10.1016/0146-6380(96)00002-2).
- Quast C, Pruesse E, Yilmaz P, Gerken J, Schweer T, Yarza P, Peplies J, Glockner FO. 2013. The SILVA ribosomal RNA gene database project: improved data processing and web-based tools. *Nucleic Acids Res* 41:D590–D596. <https://doi.org/10.1093/nar/gks1219>.
- Goris T, Schubert T, Gadkari J, Wubet T, Tarkka M, Buscot F, Adrian L, Diekert G. 2014. Insights into organohalide respiration and the versatile catabolism of *Sulfurospirillum multivorans* gained from comparative genomics and physiological studies. *Environ Microbiol* 16:3562–3580. <https://doi.org/10.1111/1462-2920.12589>.
- Ross DE, Marshall CW, May HD, Norman RS. 2016. Comparative genomic analysis of *Sulfurospirillum cavolei* MES reconstructed from the metagenome of an electrosynthetic microbiome. *PLoS One* 11:e0151214. <https://doi.org/10.1371/journal.pone.0151214>.
- Durand S, Guillier M. 2021. Transcriptional and post-transcriptional control of the nitrate respiration in bacteria. *Front Mol Biosci* 8:667758. <https://doi.org/10.3389/fmolb.2021.667758>.
- Goris T, Diekert G. 2016. The genus *Sulfurospirillum*, p 209–234. In Adrian L, Löffler FE (ed), *Organohalide-Respiring Bacteria*. Springer-Verlag Berlin Heidelberg.
- Glass JB, Ranjan P, Kretz CB, Nunn BL, Johnson AM, Xu M, McManus J, Stewart FJ. 2021. Microbial metabolism and adaptations in Atribacteria-dominated methane hydrate sediments. *Environ Microbiol* 23:4646–4660. <https://doi.org/10.1111/1462-2920.15656>.
- Yan T, Ye Q, Zhou J, Zhang CL. 2006. Diversity of functional genes for methanotrophs in sediments associated with gas hydrates and hydrocarbon seeps in the Gulf of Mexico. *FEMS Microbiol Ecol* 57:251–259. <https://doi.org/10.1111/j.1574-6941.2006.00122.x>.
- Apprill A. 2017. Marine animal microbiomes: toward understanding host-microbiome interactions in a changing ocean. *Front Mar Sci* 4:222. <https://doi.org/10.3389/fmars.2017.00222>.
- Kruse S, Goris T, Westermann M, Adrian L, Diekert G. 2018. Hydrogen production by *Sulfurospirillum* species enables syntrophic interactions of Epsilonproteobacteria. *Nat Commun* 9:4872. <https://doi.org/10.1038/s41467-018-07342-3>.
- van der Stel A-X, Wösten MMSM. 2019. Regulation of respiratory pathways in Campylobacterota: a review. *Front Microbiol* 10:1719. <https://doi.org/10.3389/fmicb.2019.01719>.

22. Huo L, Yang Y, Lv Y, Li X, Löffler FE, Yan J. 2020. Complete genome sequence of *Sulfurospirillum* strain ACS TCE, a tetrachloroethene-respiring anaerobe isolated from contaminated soil. *Microbiol Resour Announc* 9:e00941-20. <https://doi.org/10.1128/MRA.00941-20>.
23. Wang W, Li Z, Zeng L, Dong C, Shao Z. 2020. The oxidation of hydrocarbons by diverse heterotrophic and mixotrophic bacteria that inhabit deep-sea hydrothermal ecosystems. *ISME J* 14:1994–2006. <https://doi.org/10.1038/s41396-020-0662-y>.
24. Mason OU, Han J, Woyke T, Jansson JK. 2014. Single-cell genomics reveals features of a *Colwellia* species that was dominant during the Deepwater Horizon oil spill. *Front Microbiol* 5:332. <https://doi.org/10.3389/fmicb.2014.00332>.
25. Kleindienst S, Herbst F-A, Stagars M, von Netzer F, von Bergen M, Seifert J, Peplies J, Amann R, Musat F, Lueders T, Knittel K. 2014. Diverse sulfate-reducing bacteria of the *Desulfosarcina/Desulfococcus* clade are the key alkane degraders at marine seeps. *ISME J* 8:2029–2044. <https://doi.org/10.1038/ismej.2014.51>.
26. Liu H, Xin Y, Xun L. 2014. Distribution, diversity, and activities of sulfur dioxygenases in heterotrophic bacteria. *Appl Environ Microbiol* 80:1799–1806. <https://doi.org/10.1128/AEM.03281-13>.
27. Gebruk A, Southward E, Kennedy H, Southward A. 2000. Food sources, behaviour, and distribution of hydrothermal vent shrimps at the Mid-Atlantic Ridge. *J Mar Biol Ass* 80:485–499. <https://doi.org/10.1017/S0025315400002186>.
28. Sanudo-Wilhelmy SA, Gomez-Consarnau L, Suffridge C, Webb EA. 2014. The role of B vitamins in marine biogeochemistry. *Annu Rev Mar Sci* 6:339–367. <https://doi.org/10.1146/annurev-marine-120710-100912>.
29. Burns RT, Pechenik JA, Biggers WJ, Scavo G, Lehman C. 2014. The B Vitamins nicotinamide (B3) and riboflavin (B2) stimulate metamorphosis in larvae of the deposit-feeding polychaete *Capitella teleta*: implications for a sensory ligand-gated ion channel. *PLoS One* 9:e109535. <https://doi.org/10.1371/journal.pone.0109535>.
30. Jang J, Forbes VE, Sadowsky MJ. 2020. Lack of evidence for the role of gut microbiota in PAH biodegradation by the polychaete *Capitella teleta*. *Sci Total Environ* 725:138356. <https://doi.org/10.1016/j.scitotenv.2020.138356>.
31. Bayer K, Busch K, Kenchington E, Beazley L, Franzenburg S, Michels J, Hentschel U, Slaby BM. 2020. Microbial strategies for survival in the glass sponge *Vazella pourtalesii*. *mSystems* 5:e00473-20. <https://doi.org/10.1128/mSystems.00473-20>.
32. Case DH, Pasulka AL, Marlow JJ, Grupe BM, Levin LA, Orphan VJ. 2015. Methane seep carbonates host distinct, diverse, and dynamic microbial assemblages. *mBio* 6:e01348-15–e01315. <https://doi.org/10.1128/mBio.01348-15>.
33. Ruff SE, Arnds J, Knittel K, Amann R, Wegener G, Ramette A, Boetius A. 2013. Microbial communities of deep-sea methane seeps at Hikurangi continental margin (New Zealand). *PLoS One* 8:e72627. <https://doi.org/10.1371/journal.pone.0072627>.
34. Jørgensen BB, Findlay AJ, Pellerin A. 2019. The biogeochemical sulfur cycle of marine sediments. *Front Microbiol* 10:849–849. <https://doi.org/10.3389/fmicb.2019.00849>.
35. Woyke T, Teeling H, Ivanova NN, Huntemann M, Richter M, Gloeckner FO, Boffelli D, Anderson LJ, Barry KW, Shapiro HJ, Szeto E, Kyrpides NC, Mussmann M, Amann R, Bergin C, Ruehland C, Rubin EM, Dubilier N. 2006. Symbiosis insights through metagenomic analysis of a microbial consortium. *Nature* 443:950–955. <https://doi.org/10.1038/nature05192>.
36. Thorsen MS, Wieland A, Ploug H, Kragelund C, Nielsen PH. 2003. Distribution, identity and activity of symbiotic bacteria in anoxic aggregates from the hindgut of the sea urchin *Echinocardium cordatum*. *Ophelia* 57:1–12. <https://doi.org/10.1080/00785236.2003.10409501>.
37. Carbonero F, Benefiel A, Alizadeh-Ghamsari A, Gaskins HR. 2012. Microbial pathways in colonic sulfur metabolism and links with health and disease. *Front Physiol* 3:448. <https://doi.org/10.3389/fphys.2012.00448>.
38. Ley RE, Hamady M, Lozupone C, Turnbaugh PJ, Ramey RR, Bircher JS, Schlegel ML, Tucker TA, Schrenzel MD, Knight R, Gordon JI. 2008. Evolution of mammals and their gut microbes. *Science (New York, NY)* 320:1647–1651. <https://doi.org/10.1126/science.1155725>.
39. Chen X, Li M, Liu H, Li B, Guo L, Meng Z, Lin H. 2016. The complete mitochondrial genome of the polychaete, *Goniada japonica* (Phyllodoceida, Goniadidae). *Mitochondrial DNA A DNA Mapp Seq Anal* 27:2850–2851. <https://doi.org/10.3109/19401736.2015.1053124>.
40. Zhang N, Song C, Wang M, Liu Y, Hui M, Cui Z. 2017. Diversity and characterization of bacteria associated with the deep-sea hydrothermal vent crab *Austinograea* sp. comparing with those of two shallow-water crabs by 16S ribosomal DNA analysis. *PLoS One* 12:e0187842. <https://doi.org/10.1371/journal.pone.0187842>.
41. Leignel V, Hurtado LA, Segonzac M. 2018. Ecology, adaptation and acclimatisation mechanisms of Bythograeidae Williams, 1980, a unique endemic hydrothermal vent crabs family: current state of knowledge. *Mar Freshw Res* 69:1–15. <https://doi.org/10.1071/MF17007>.
42. Gruber-Vodicka HR, Seah BKB, Priesse E. 2020. phyloFlash: rapid small-subunit rRNA profiling and targeted assembly from metagenomes. *mSystems* 5:e00920-20. <https://doi.org/10.1128/mSystems.00920-20>.
43. Li D, Luo R, Liu CM, Leung CM, Ting HF, Sadakane K, Yamashita H, Lam TW. 2016. MEGAHIT v1.0: a fast and scalable metagenome assembler driven by advanced methodologies and community practices. *Methods* 102:3–11. <https://doi.org/10.1016/j.ymeth.2016.02.020>.
44. Eren AM, Kiefl E, Shaiber A, Veseli I, Miller SE, Schechter MS, Fink I, Pan JN, Yousef M, Fogarty EC, Trigodet F, Watson AR, Esen ÖC, Moore RM, Clayssen Q, Lee MD, Kivenson V, Graham ED, Merrill BD, Karkman A, Blankenberg D, Eppley JM, Sjödin A, Scott JJ, Vázquez-Campos X, McKay LJ, McDaniel EA, Stevens SLR, Anderson RE, Fuessel J, Fernandez-Guerra A, Maignien L, Delmont TO, Willis AD. 2021. Community-led, integrated, reproducible multi-omics with anvio. *Nat Microbiol* 6:3–6. <https://doi.org/10.1038/s41564-020-00834-3>.
45. Parks DH, Imelfort M, Skennerton CT, Hugenholtz P, Tyson GW. 2015. CheckM: assessing the quality of microbial genomes recovered from isolates, single cells, and metagenomes. *Genome Res* 25:1043–1055. <https://doi.org/10.1101/gr.186072.114>.
46. Chaumeil P-A, Mussig AJ, Hugenholtz P, Parks DH. 2019. GTDB-Tk: a toolkit to classify genomes with the Genome Taxonomy Database. *Bioinformatics* 36:1925–1927. <https://doi.org/10.1093/bioinformatics/btz848>.
47. Al-Shayeb B, Schoelmerich MC, West-Roberts J, Valentin-Alvarado LE, Sachdeva R, Mullen S, Crits-Christoph A, Wilkins MJ, Williams KH, Doudna JA, Banfield JF. 2021. Borgs are giant extrachromosomal elements with the potential to augment methane oxidation. *bioRxiv* <https://doi.org/10.1101/2021.07.10.451761>.
48. Zhou Z, Tran P, Liu Y, Kieft K, Anantharaman K. 2019. METABOLIC: a scalable high-throughput metabolic and biogeochemical functional trait profiler based on microbial genomes. *bioRxiv* <https://doi.org/10.1101/761643>.
49. Overbeek R, Olson R, Pusch GD, Olsen GJ, Davis JJ, Disz T, Edwards RA, Gerdes S, Parrello B, Shukla M, Vonstein V, Wattam AR, Xia F, Stevens R. 2014. The SEED and the rapid annotation of microbial genomes using subsystems technology (RAST). *Nucleic Acids Res* 42:D206–D214. <https://doi.org/10.1093/nar/gkt1226>.
50. Altschul SF, Gish W, Miller W, Myers EW, Lipman DJ. 1990. Basic local alignment search tool. *J Mol Biol* 215:403–410. [https://doi.org/10.1016/S0022-2836\(05\)80360-2](https://doi.org/10.1016/S0022-2836(05)80360-2).
51. Johnson M, Zaretskaya I, Raytselis Y, Merezukh Y, McGinnis S, Madden TL. 2008. NCBI BLAST: a better web interface. *Nucleic Acids Res* 36:W5–W9. <https://doi.org/10.1093/nar/gkn201>.
52. Callaghan AV, Morris BE, Pereira IA, McInerney MJ, Austin RN, Groves JT, Kukor JJ, Sufliya JM, Young LY, Zylstra GJ, Wawrik B. 2012. The genome sequence of *Desulfatibacillum alkenivorans* AK-01: a blueprint for anaerobic alkane oxidation. *Environ Microbiol* 14:101–113. <https://doi.org/10.1111/j.1462-2920.2011.02516.x>.
53. Caspi R, Billington R, Keseler IM, Kothari A, Krummenacker M, Midford PE, Ong WK, Paley S, Subhraveti P, Karp PD. 2020. The MetaCyc database of metabolic pathways and enzymes - a 2019 update. *Nucleic Acids Res* 48:D445–D453. <https://doi.org/10.1093/nar/gkz862>.